

# 特高压直流控制保护系统相位光时域反射仪信噪比提升方法

阮峻<sup>1</sup>, 朱志俊<sup>1</sup>, 孙豪<sup>1</sup>, 朱一峰<sup>1</sup>, 徐宛丽<sup>2</sup>, 吕涛<sup>2</sup>, 吴宝锋<sup>2</sup>, 孙小茵<sup>2\*</sup>

<sup>1</sup>中国南方电网超高压输电公司昆明局, 云南 昆明 650300;

<sup>2</sup>东南大学光传感/通信综合网络国家地方联合工程研究中心, 江苏 南京 210096

**摘要** 分析了由特高压直流输电控制保护工程系统相位光时域反射仪( $\Phi$ -OTDR)测得光缆沿线时域、频域信号的分布规律,提出了信号时域乘法短时过双电平率与频域分段频带均方根误差(RSM)综合算法,编制了综合算法程序,开展了工程实验。当光缆链路在 2.3,5.0,10.8,16.0 km 处存在微弱故障时,利用乘法短时过双电平率法可使系统信噪比(SNR)分别提高到 9.41 dB,9.02 dB,7.60 dB,3.50 dB。当光缆链路信号频带内分段数为 8 时,系统 SNR 可进一步提升,且频带 RSM 峰值可突出微弱故障位置,与实际情况差异小。所提方法的光缆链路微弱故障定位精度达到 $\pm 2$  m,不仅提升了工程系统的 SNR,还解决了难以辨识光缆链路微弱故障的问题。

**关键词** 光纤光学; 特高压; 直流控制保护; 相位光时域反射仪( $\Phi$ -OTDR); 信噪比(SNR)

**中图分类号** O436 **文献标志码** A

**DOI:** 10.3788/CJL202249.0906005

## 1 引言

在“西电东送”项目的实施过程中,特高压直流输电工程的优势凸显。特高压直流控制保护系统中应用了控制、直流测量及避雷等多类光纤光缆,与光纤连接器构成光缆链路。实际运行中,只要这类光缆链路发生微弱故障,都会给系统带来极大风险<sup>[1]</sup>。传统的光时域反射仪(OTDR)以信号幅值为特征参数进行时、空域处理,原理简单且实时性强,可及时发现系统存在的较大故障<sup>[2-4]</sup>,但信噪比(SNR)低,难以辨识光缆链路存在的微弱故障<sup>[5-6]</sup>。以时、频域为尺度的小波去噪法可适度提高系统的 SNR<sup>[7-9]</sup>,但计算复杂、实时性差、环境适应性弱,仍难以辨识微弱故障。

采用相位光时域反射仪( $\Phi$ -OTDR)可辨识链路存在的微弱故障,灵敏度较高,且计算复杂度降低<sup>[10-13]</sup>。本课题组已在实验室内搭建了光纤链路系统,模拟了特高压直流输电工程控制保护系统关键元部件故障状态及环境信息,获得并分析了  $\Phi$ -OTDR 底层时域背向散射相位调制信息,并提出一

种对光纤链路微弱故障乘积分段信息熵定位算法,提高了定位精度<sup>[14]</sup>。但是,将该技术用于实际特高压直流输电工程控制保护系统中,工程现场环境对光缆链路的影响较大,导致系统终端接收信号的信噪比太低,微弱故障信号被淹没在其中,难以区分与获知。因此,必须探究实际工程系统的信号特征,找出降低噪声的途径,优化去噪算法,提升 SNR,从而达到准确定位系统微弱故障的目的。

本文在已搭建的特高压直流输电控制保护工程系统上,根据  $\Phi$ -OTDR 端机实测结果,分析了信号时、频域特征,提出一种时域信号乘法短时过双电平率与频域信号分段频带标准差处理综合算法,并计算了该算法对系统 SNR 的提升结果。

## 2 系统原理与实测信号分析

图 1(a)、(b)分别给出  $\Phi$ -OTDR 光缆链路故障检测原理和端机设备照片。 $\Phi$ -OTDR 系统与文献<sup>[14]</sup>所提系统相同,由光发送模块、光纤干涉仪、检测光缆、光接收模块、模拟微弱故障源、信号处理模

收稿日期: 2021-09-06; 修回日期: 2021-10-02; 录用日期: 2021-10-21

基金项目: 国家自然科学基金(61271206)、南方电网 2019 年科技服务项目(2019-41)

通信作者: \*xhsun@seu.edu.cn

块等组成。由光发送模块发出的检索光脉冲进入光缆链路,受微弱故障扰动,导致光缆链路背向散射光相位发生变化,通过光纤干涉仪将其转变为光强度

信号,从而得知故障位置。检测光缆从终端设备接出,通过外接光缆接口用于实际特高压直流输电控制保护系统中。

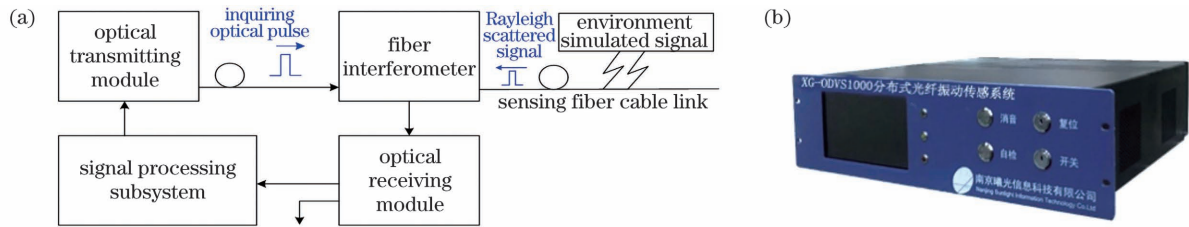


图 1  $\Phi$ -OTDR 系统。(a)原理框图;(b)端机设备照片

Fig. 1  $\Phi$ -OTDR system. (a) Functional block diagram; (b) photo of terminal equipment

图 2 所示为特高压直流控制保护工程系统测试环境与实测信号。图 2(a)~(d)分别为特高压直流控制保护系统中敷设在换流站的感知光缆、控制保护系统光缆接口、安装在主控室内的  $\Phi$ -OTDR 终端设备和示波器显示的链路波形。端机设备参数如下:检索脉冲脉宽为  $1 \mu\text{s}$ ,峰值功率为  $18 \text{ mW}$ ,重复频率为  $1 \text{ kHz}$ ,光缆链路长度为  $18 \text{ km}$ ;在信号处理

子系统 FPGA 板卡中预留了输出接口,可通过示波器观测光缆链路信号。图 2(d)所示为在光缆链路  $2.3 \text{ km}$  附近(换流站某节点)施加扰动,采集 30 个检索周期内原始信号经示波器的输出结果,方框标出故障信号可能出现的位置。可见,换流站工作环境复杂,沿线光缆均工作在振动环境中,故障信号的 SNR 低,且时间窗口过大。

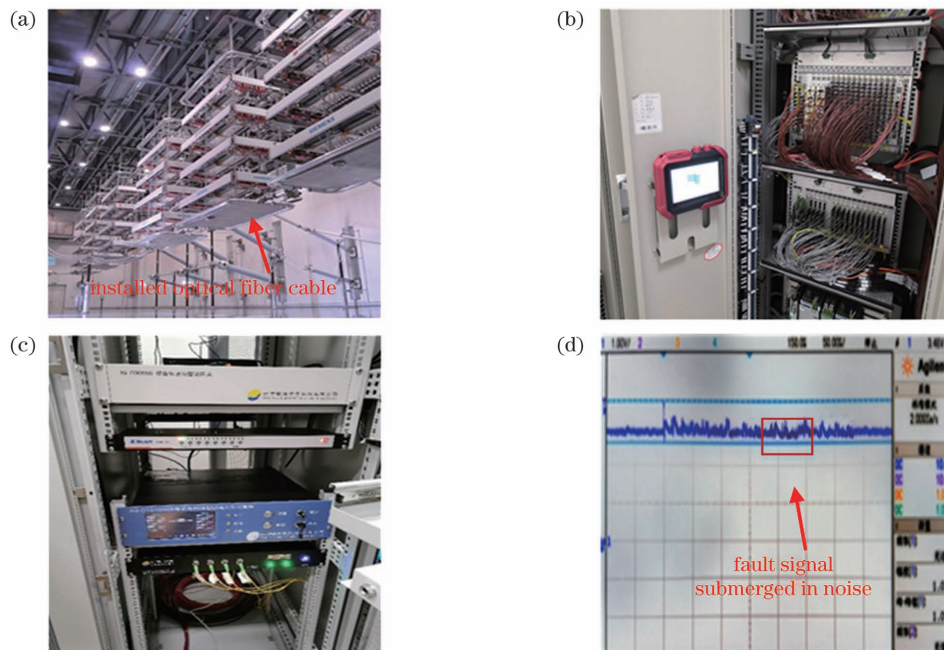


图 2 特高压直流控制保护工程系统光缆链路测试环境与信号。(a)安装了光缆链路的换流阀;(b)控制保护系统光缆接口;(c)安装在机柜中的  $\Phi$ -OTDR 端机;(d)示波器输出的实测信号

Fig. 2  $\Phi$ -OTDR test environment and signal in ultra-high voltage direct current control and protection system.

(a) Converter with optical fiber cable link; (b) optical fiber cable interface on the control and protection system;

(c)  $\Phi$ -OTDR terminal equipment placed in cabinet; (d) measurement signal displayed by oscilloscope

经过多次重复实验,分析由  $\Phi$ -OTDR 端机设备底层 FPGA 高速数据采集卡获得的光缆链路数据特征,发现故障信号时域特征参数统计特性满足一定规律,但与噪声信号的统计规律有较大差别。因此,通过特征参数可提升光缆链路故障信号的 SNR。实测

结果还发现,光缆链路噪声频谱和故障信号频谱的分布特点不同,前者分布均匀,后者集中在振动主频处且离散度较大。因此,根据光缆链路噪声频谱和故障信号频谱的分布特性差异,可在提升光缆链路故障信号 SNR 的同时,找出故障区域,实现故障精准定位。

### 3 信噪比提升算法

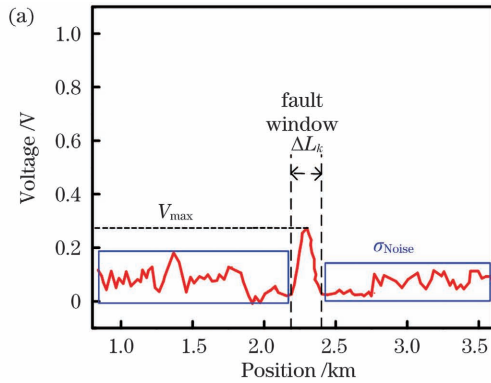
#### 3.1 时域信号乘法短时过双电平率

由于光缆链路沿线均受环境影响,信号噪声较大,微弱故障偶然出现,因此提取信号特征时要避免信号噪声的干扰。将短时过电平率  $Z_v$  定义为一定采样周期内相邻两个采样点数值相对阈值电平符号发生改变的频率,反映了一段信号在某个先验值附近变化快慢的细节信息。 $Z_v$  可表示为

$$Z_v = \frac{1}{2M} \sum_{i=1}^{M-1} | \operatorname{sgn}[x(i+1) - V] - \operatorname{sgn}[x(i) - V] |, \quad (1)$$

式中: $i$ 、 $M$  分别为采集信号的周期数和最大周期数; $x(i)$  为信号幅值; $\operatorname{sgn}$  为符号函数,即

$$\operatorname{sgn}[x(i)] = \begin{cases} 1, & x(i) \geq 0 \\ -1, & x(i) < 0 \end{cases} \quad (2)$$



首先讨论阈值电平与采样周期。分别采集系统工作条件不变、2.3 km 处存在微弱故障时光缆链路在 10, 20, 30, …, 80 个周期内感知信号的平均值,形成平均滤波后整条光缆链路的信号曲线,结果见图 3(a),其中  $V_{\max}$  为整条光缆链路信号的电压极值。根据沿光缆链路 SNR 的定义<sup>[15]</sup>,可得到 SNR 的对数表示式为

$$\xi_{\text{SNR}} = 10 \lg \frac{V_{\max}}{\sigma_{\text{Noise}}}, \quad (3)$$

式中: $\xi_{\text{SNR}}$  的单位为 dB; $\sigma_{\text{Noise}}$  为噪声信号方差。

当阈值电平  $V$  分别取  $V_{\max}/4$ 、 $V_{\max}/2$ 、 $3V_{\max}/4$ 、 $V_{\max}$  时,计算信号短时过电平率,得到 SNR 的变化情况,结果见图 3(b)。可见,链路 SNR 在采集周期大于 20 后变化不明显,系统 SNR 在阈值电平为  $3V_{\max}/4$  时最大。因此,确定最大周期数为 30,阈值电平为  $3V_{\max}/4$ 。

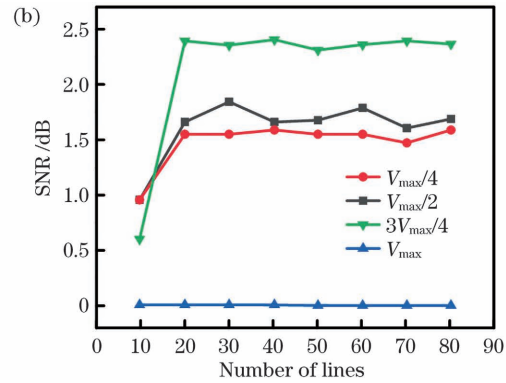


图 3 阈值电平与采样周期信号处理结果。(a) 阈值电平;(b) SNR 与采样周期的关系

Fig. 3 Threshold level and sampling period signal processing results. (a) Threshold level; (b) relationship between SNR and number of sampling cycles

为了提高光缆链路微弱故障信号的 SNR,将短时过双阈值电平作为评判条件,可滤除更多噪声。分别设置上、下阈值电平为  $V_1$ 、 $V_2$  ( $V_1 > V_2$ ),定义对应的短时过上、下阈值电平率为  $Z_{V_1}$ 、 $Z_{V_2}$ ,按照式(1), $Z_{V_1}$ 、 $Z_{V_2}$  分别表示为

$$Z_{V_1} = \frac{1}{2M} \sum_{i=1}^{M-1} | \operatorname{sgn}[x(i+1) - V_1] - \operatorname{sgn}[x(i) - V_1] |, \quad (4)$$

$$Z_{V_2} = \frac{1}{2M} \sum_{i=1}^{M-1} | \operatorname{sgn}[x(i+1) - V_2] - \operatorname{sgn}[x(i) - V_2] |. \quad (5)$$

统计光缆链路沿线信号穿越上、下阈值的频率,定义加法短时过双电平率为短时过上电平率与短时过下电平率之和:

$$Z_{(V_1, V_2)} = Z_{V_1} + Z_{V_2}. \quad (6)$$

加法短时过双电平率法在故障信号与噪声信号

幅值相差较小时,经过信号处理后会出干扰。为有效降低干扰,定义乘法短时过双电平率为上、下阈值电平率之积:

$$Z_{(V_1, V_2)}^1 = Z_{V_1} Z_{V_2}. \quad (7)$$

考虑到阈值电平  $V$  可能存在负值,为便于计算,各位置处的信号电平按式(8)作减法处理:

$$x(i) = x(i) - \sum_{i=1}^M x(i) / M. \quad (8)$$

#### 3.2 频带均方根差法

对系统采集信号进行频域分析,发现故障信号频谱强度分布为:主频率处强度较大,其他频率分量分布均匀,分布离散度较大;噪声信号频谱分布均匀,离散度较小。因此,通过傅里叶变换,将光缆链路信号频谱分成不同的频带,可由频带均方根误差(RSMD)判断检测链路上有无故障。

设频谱强度  $P$  由  $P_{\omega_1}$ 、 $P_{\omega_2}$ 、…、 $P_{\omega_N}$  组成,即

$P = \{P(\omega_1), P(\omega_2), \dots, P(\omega_i), \dots, P(\omega_N)\}, i = 1, \dots, N$ , 其中  $P(\omega_i)$  分量定义为信号功率谱中频率满足  $\omega_{i-1} \leq f < \omega_i$  时子频带功率和, 即

$$P(\omega_i) = \sum_{f=\omega_{i-1}}^{\omega_i} p(f). \quad (9)$$

式(9)表示将光缆链路信号全频谱均分为  $N$  个频带后第  $i$  个频带的功率分量, 其均值为

$$E = \frac{1}{N} \sum_{i=1}^N P(\omega_i). \quad (10)$$

频带的 RSMD 为

$$\sigma_N = \sqrt{\frac{1}{N} \sum_{i=1}^N [P(\omega_i) - E]^2}. \quad (11)$$

基于以上算法给出图 4 所示光缆链路 SNR 计算流程。首先, 对工程系统采样 30 个周期信号平均滤波后的链路信号, 采用式(4)和式(5)获得时域短时上、下过电平率, 并按式(8)进行减法处理; 其次, 基于式(7)计算乘法短时过双电平率, 再依据式(11)计算频带的 RSMD; 然后, 按照式(3)计算出 SNR, 获得光缆链路沿线故障窗口区域与 SNR 分布; 最后, 采用文献[14]的算法实现故障定位。

### 4 结果与讨论

在图 2 给出的特高压直流控制保护工程系统中开展实验, 进行结果分析。

#### 4.1 时域信号 3 种过电平率信号处理结果与分析

当光缆链路 2.3 km 处存在微弱故障时, 以 30 个周期信号平均滤波后构成链路信号曲线, 采集 100 条曲线, 对原始信号按照式(8)进行减法处理后得到图5(a)所示的结果。分别计算故障信号短时过

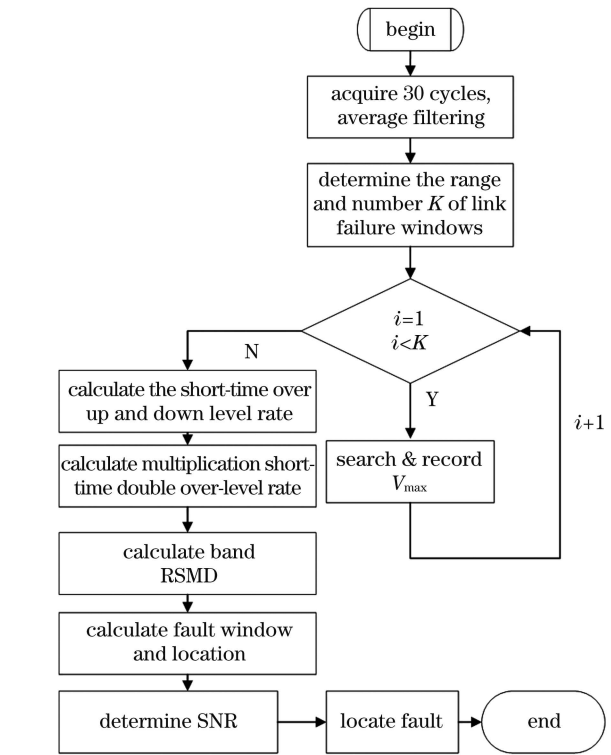
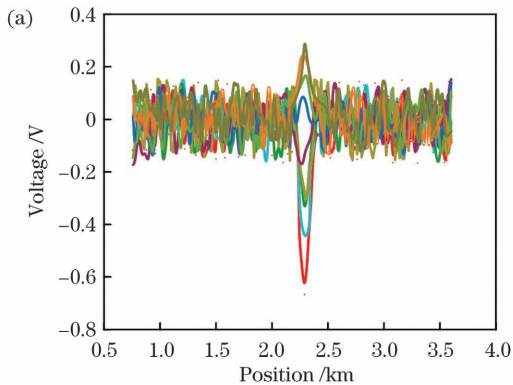


图 4 光缆链路 SNR 确定和故障定位流程

Fig. 4 Flow chart of optical cable link SNR and fault location

电平率、加法短时过双电平率, 得到其随检测位置的分布情况, 见图 5(b)。可以看到, 非故障位置处信号短时过电平率与加法短时过双电平率为 0, 故障位置处信号短时过电平率与加法短时过双电平率突变, 且故障位置处信号加法短时过双电平率相较于短时过电平率从 0.5 提高至 0.8。可见, 加法短时过电平率方法的处理结果优于短时过电平率方法。

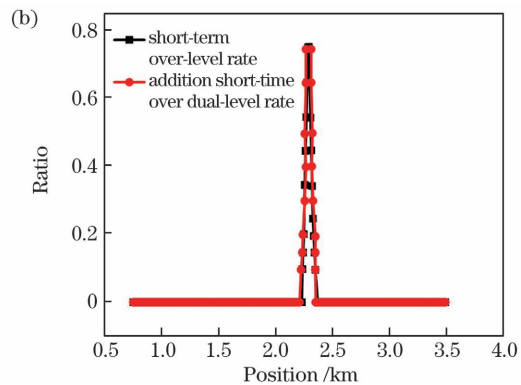


图 5 加法短时过双电平率法的信号处理结果。(a)原始信号经式(8)减法处理的结果;(b)两种算法的结果对比

Fig. 5 Results of addition short-time over double-level rate method. (a) Results of original signal subtraction processing by Eq. (8); (b) comparison of results by two algorithms

当光缆链路在 10.8 km 附近存在微弱故障时, 有、无故障的位置处加法短时过电平率分别为 0.55、0.23, SNR 下降明显, 需采用乘法短时过双电

平率方法处理信号。以 30 个周期信号平均滤波后构成链路信号曲线, 采集 100 条曲线, 对原始信号按照式(8)进行减法处理后得到图6(a)所示的结果,

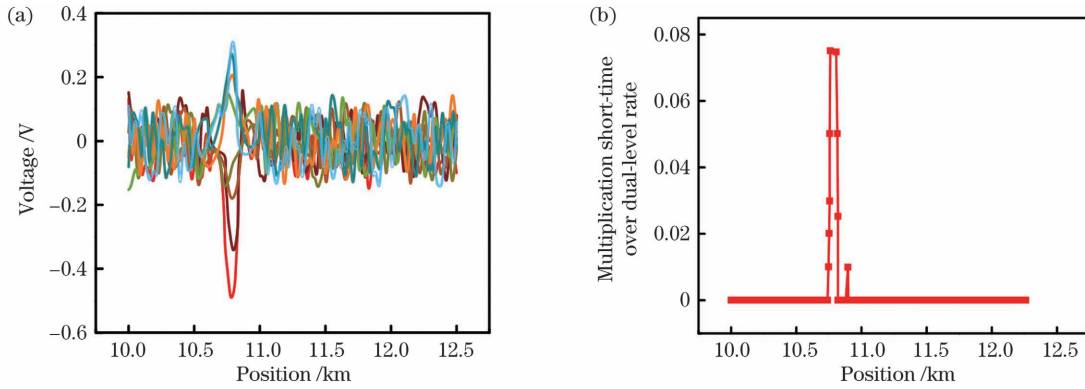


图 6 乘法短时过双电平率方法的信号处理结果。(a)原始信号经式(8)减法处理的结果;(b)故障信号乘法短时过双电平率

Fig. 6 Results of multiplication short-time over double-level rate method. (a) Results of original signal subtraction processing by Eq. (8); (b) fault signal multiplication short-time over two-level rate

乘法短时过双电平率随链路位置分布情况如图 6(b)所示。有、无故障位置处乘法短时过双电平率分别为 0.08、0.01, 系统 SNR 达到 7.60 dB。

工程系统测试环境中,当光缆链路在 2.3, 5.0, 10.8, 16.0 km 处分别存在微弱故障时,选取 30 个周期信号平均滤波后构成链路信号曲线,采集 100 根曲线,分别采用短时过电平率、加法短时过双电平率、乘法短时过双电平率方法进行信号处理,得到系统 SNR 随微弱故障位置的分布情况,如图 7 所示。可见,与原始信号相比,短时过电平率方法在链路长度较短(2.3 km、5.0 km)时 SNR 较高,但随着链路长度的增大,SNR 仅缓慢增加,难以分辨故障信号。加法短时过双电平率方法将系统 SNR 提升至小于 3 dB;乘法短时过双电平率方法在 2.3, 5.0, 10.8, 16.0 km 故障位置处,系统 SNR 由 2.80 dB、1.10 dB、0.80 dB、0.25 dB 分别提升到 9.41 dB、9.00 dB、7.60 dB、3.50 dB,且随着故障位置与端机出口的距离

增大,SNR 增值减小。两种算法产生差异原因在于有、无故障处过双电平率的计算方法不同。由于故障位置处信号波动较大,上、下过阈值率均不等于 0;而非故障位置处信号波动较小,可能只有上过阈值率,下过阈值为 0。短时加法过双电平率则等于短时上过阈值率,但短时乘法过双电平率则为 0。综上,乘法短时过双电平率大大降低了噪声,提升了系统 SNR,且可找出光缆链路故障信号区域。

#### 4.2 频带均方根法信号处理结果与分析

针对系统光缆链路 2.3 km 处存在故障的状况,取 0.75~3.5 km 段信号,利用快速傅里叶变换获得 64 个子频带的频谱,得到取不同  $N$  时频带 RSMD 随信号位置的分布情况,如图 8(a)所示。可以看到,非故障位置处信号频带标准差在 0.2 附近波动,2.3 km 处信号频带的 RSMD 突变,且其峰值与  $N$  值有关。当  $N$  为 8 时,频带 RSMD 约为 6,达到最大值,其峰值对应的位置与实际故障位置非常接近。当  $N$  为 1、32 时,频带 RSMD 约为 1.2。不同  $N$  值时系统 SNR 的分布见图 8(b),系统 SNR 随着  $N$  的增大先增大后减小,当  $N=8$  时,系统 SNR 达到最大值 9.80 dB。可见,系统 SNR 随  $N$  的变化关系与频带 RSMD 随  $N$  的变化关系一致,且频带分段数存在最佳值。这是因为由光缆链路微弱故障引起的背向散射信号频带较窄, $N$  过大,主频频谱离散过多,其频带 RSMD 反而会降低。

按照图 4 所示流程编制了工程系统信号处理程序,发现光缆链路微弱故障定位精度达到  $\pm 2$  m。

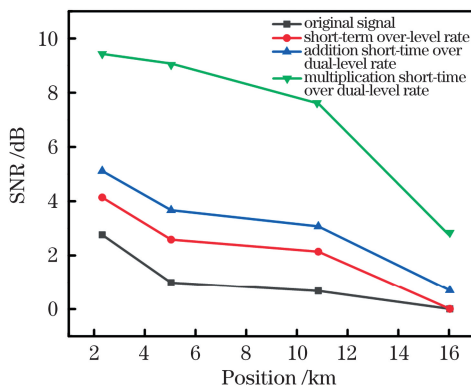


图 7 三种算法对时域信号的处理结果对比

Fig. 7 Comparison of processing results for time-domain signal by three algorithms

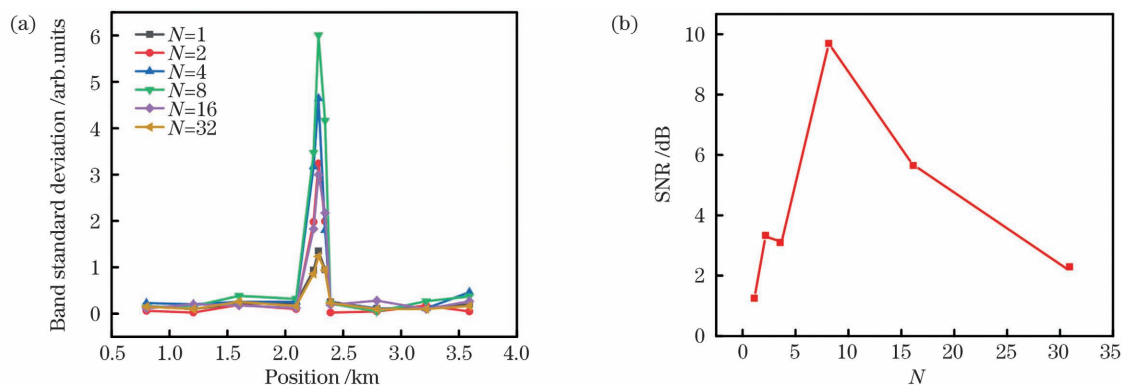


图 8 信号频带经 RSMD 法处理的结果。(a)不同位置处信号频带标准差;(b)SNR 与带内分段数的关系  
Fig. 8 Signal processing results of frequency band by RSMD method. (a) Signal frequency band standard deviation at different positions; (b) relationship between SNR and in-band segmentation number

## 5 结 论

基于特高压直流控制保护系统搭建的  $\Phi$ -OTDR 现场测试环境,分析了系统光缆沿线时、频域信号特征与统计规律,给出了时域信号短时过零率、加法短时过双电平率表征方式,提出一种时域信号乘法短时过双电平率与频域信号分段频带 RSMD 相结合的算法。时域信号分析与处理结果表明,乘法短时过双电平率方法的处理效果最佳, $\Phi$ -OTDR 系统在光缆链路 2.3, 5.0, 10.8, 16.0 km 位置故障条件下,系统 SNR 分别提高到 9.41 dB、9.02 dB、7.60 dB、3.50 dB。频域信号分析与处理方法的结果表明, $\Phi$ -OTDR 系统在光纤链路 2.3 km 位置故障条件下,当  $N=8$  时,系统 SNR 进一步提升,且频带 RSMD 峰值可突出微弱故障位置,与实际情况差异小。两种算法相结合,可使得信号处理耗时短,光缆链路微弱故障定位精度达到  $\pm 2$  m。所提算法提升了工程系统  $\Phi$ -OTDR 检测信号的 SNR,实现了微弱故障的精确定位。

## 参 考 文 献

- [1] 刘振亚, 秦晓辉, 赵良, 等. 特高压直流分层接入方式在多馈入直流电网的应用研究[J]. 中国电机工程学报, 2013, 33(10): 1-7, 25.  
Liu Z Y, Qin X H, Zhao L, et al. Study on the application of UHVDC hierarchical connection mode to multi-infeed HVDC system[J]. Proceedings of the CSEE, 2013, 33(10): 1-7, 25.
- [2] Feng Q G, Li W, Zheng Q, et al. The OTDR with high dynamic range based on LFM signal and FDM[J]. IEEE Photonics Technology Letters, 2020, 32(7): 359-362.
- [3] Amaral G C, Garcia J D, Herrera L E Y, et al. Automatic fault detection in WDM-PON with tunable photon counting OTDR [J]. Journal of Lightwave Technology, 2015, 33(24): 5025-5031.
- [4] Wang D, Zou J, Wang Y, et al. Distributed optical fiber low-frequency vibration detecting using cross-correlation spectrum analysis [J]. Journal of Lightwave Technology, 2020, 38(23): 6664-6670.
- [5] Wang L Q, Yi X G, Zhang J G, et al. Impact of chromatic dispersion on the performance of COTDR [J]. IEEE Photonics Technology Letters, 2016, 28(13): 1418-1421.
- [6] Xiong B H, Luo X S, Gu J, et al. A POTDR system based on dual sensing directions[J]. IEEE Photonics Journal, 2020, 12(2): 1-8.
- [7] Maraval D, Gabet R, Jaouen Y, et al. Dynamic optical fiber sensing with Brillouin optical time domain reflectometry: application to pipeline vibration monitoring [J]. Journal of Lightwave Technology, 2017, 35(16): 3296-3302.
- [8] Martins H F, Martin-Lopez S, Corredera P, et al. Distributed vibration sensing over 125 km with enhanced SNR using Phi-OTDR over a URFL cavity [J]. Journal of Lightwave Technology, 2015, 33(12): 2628-2632.
- [9] 王放, 邢冀川. 一种新型智能化远距光纤预警的算法研究[J]. 光学学报, 2021, 41(7): 0706002.  
Wang F, Xing J C. Novel intelligent long-distance optical fiber pre-warning algorithm [J]. Acta Optica Sinica, 2021, 41(7): 0706002.
- [10] Bai Q, Xue B, Gu H, et al. Enhancing the SNR of BOTDR by gain-switched modulation [J]. IEEE Photonics Technology Letters, 2019, 31(4): 283-286.
- [11] Zhu H, Pan C, Sun X H. Vibration pattern recognition and classification in OTDR based distributed optical-fiber vibration sensing system[J]. Proceedings of SPIE, 2014, 9062: 906205.

- [12] 宋牟平, 庄守望, 王轶轩. 相位敏感光时域反射计的高频振动检测[J]. 中国激光, 2020, 47(5): 0506001. Song M P, Zhuang S W, Wang Y X. High-frequency vibration detection of phase-sensitive optical time-domain reflectometer[J]. Chinese Journal of Lasers, 2020, 47(5): 0506001.
- [13] 盛庆华, 俞钊, 卢斌, 等. 基于异构加速的  $\Phi$ -OTDR 实时信号处理系统[J]. 中国激光, 2020, 47(1): 0104002. Sheng Q H, Yu Z, Lu B, et al. Real-time phase-sensitive optical time-domain reflectometry signal processing system based on heterogeneous accelerated computing[J]. Chinese Journal of Lasers, 2020, 47(1): 0104002.
- [14] 阮峻, 孙豪, 朱志俊, 等. 直流控保系统光纤链路微弱故障的定位[J]. 中国激光, 2021, 48(20): 2006002. Ruan J, Sun H, Zhu Z J, et al. Location of weak faults in optical fiber links of direct current control and protection system[J]. Chinese Journal of Lasers, 2021, 48(20): 2006002.
- [15] Bentz C M, Baudzus L, Krummrich P M. Signal to noise ratio (SNR) enhancement comparison of impulse-, coding- and novel linear-frequency-chirp-based optical time domain reflectometry (OTDR) for passive optical network (PON) monitoring based on unique combinations of wavelength selective mirrors [J]. Photonics, 2014, 1(1): 33-46.

## SNR Improvement Methods for Phase-Sensitive Optical Time-Domain Reflectometer for UHV DC Control and Protection System

Ruan Jun<sup>1</sup>, Zhu Zhijun<sup>1</sup>, Sun Hao<sup>1</sup>, Zhu Yifeng<sup>1</sup>, Xu Wanli<sup>2</sup>, Lü Tao<sup>2</sup>,  
Wu Baofeng<sup>2</sup>, Sun Xiaohan<sup>2\*</sup>

<sup>1</sup> Kunming Bureau, CSG EHV Power Transmission Company, Kunming 650300, Yunnan, China;

<sup>2</sup> National Research Center for Optical Sensing/Communications Integrated Networking, Southeast University, Nanjing 210096, Jiangsu, China

### Abstract

**Objective** Many optical-fiber cables with properties, such as control, DC measurement, and lightning protection are applied in the UHV DC control and protection system, forming an optical cable link with optical cable connectors. In actual operation, the weak failure of optical cable links brings great risks to the system. Phase-sensitive optical time-domain reflectometry ( $\Phi$ -OTDR) detects and locates the faults along the optical cable link. However, when  $\Phi$ -OTDR is used in an actual UHV DC engineering system, the site environment greatly impacts the optical cable link, resulting in a very low signal-to-noise ratio (SNR) of the received signal at the system terminal. So, the weak fault signal is submerged in noise and difficult to distinguish. In this study, we explore the signal characteristics of the actual engineering system and find ways to reduce noise, optimize the denoising algorithm, and improve SNR, to achieve accurate positioning of weak faults in the system.

**Methods**  $\Phi$ -OTDR-based test environment is established in the UHV DC control and protection engineering system. We analyze the data characteristics of the optical cable link obtained using the high-speed data acquisition card at the bottom of  $\Phi$ -OTDR terminal equipment after repeated experiments. Results show that the statistical characteristics of time-domain characteristic parameters of fault signal meet a certain law, different from the statistical law of noise signal. Also, the distribution of noise spectrum and fault signal spectrum density of the optical cable link is different. The former has uniform performance and the latter concentrates on the main vibration frequency with large dispersions. Thus, given the frequency domain-segmented band root mean square difference (RSMD) and algorithm flow, we propose a synthesis algorithm of time-domain multiplication short-time over dual-level rate.

**Results and Discussions** The comprehensive algorithm program and experiment are compiled and conducted in the UHV DC control and protection engineering system. Given a weak fault at 2.3 km of optical cable link, the original signal is subtracted. The short-time over-level rate and addition short-time over-level rate of the signal at the non-fault position are zero. Also, the short-time over-level rate and addition short-time over-level rate of the signal at the fault position change, and the ratio of the short-time over-level rate of the signal at the fault position increases from

0.5 to 0.8. The addition short-time over-level rate is better than the short-time over-level rate (Fig. 5). Given a weak fault near a 10.8 km optical cable link, the addition short-time over-level rate at that position with and without fault is 0.55 and 0.23, respectively, and the SNR decreases. Therefore, the multiplication short-time over dual-level rate should be used to process the signal as 0.08 and 0.01, respectively, thereby achieving a system SNR of 7.60 dB (Fig. 6).

With weak faults at 2.3, 5.0, 10.8, and 16.0 km of optical cable links in the engineering system test environment, 30 periodic signals are averaged filtered to form link signal curves, and 100 curves are collected. The signal processing is performed using the short-time over-level rate, addition short-time over-level rate, and multiplication short-time over dual-level rate, respectively. Also, the distribution of system SNR with weak fault locations is obtained. The multiplication of short-time over dual-level rate greatly reduces noise and improves the system SNR (Fig. 7).

Due to the fault at 2.3 km of the optical cable link of the system, we obtain the frequency spectrum of 64 sub-bands from the signal ranging from 0.75 to 3.5 km using the fast Fourier transform and the distribution of frequency band RSMD with the signal position at  $N$  different times (Fig. 8). The standard deviation of the signal band at the non-fault location fluctuates around 0.2, the RSMD of the signal band at 2.3 km changes, with its peak value related to the  $N$  value. The SNR of the system increases first and then decreases as  $N$  increases. When  $N=8$ , the frequency band RSMD is approximately equal to 6 and the system SNR reaches 9.80 dB, reaching the maximum value. The difference between the corresponding peak position and the actual fault location is very small.

**Conclusions** From the  $\Phi$ -OTDR test environment built in the UHV DC control and protection engineering system, we analyze the characteristics and statistical law for fault detection signal in both the frequency and time domains along the optical cable link. The expressions of short-time over-level rate and addition short-time over dual-level rate for the signal in the time domain are given. Furthermore, we propose a synthesis algorithm of the time-domain multiplication short-time over dual-level rate and frequency domain-segmented band RSMD. Results show that the short-time dual-level rate is the best, and the SNR of the  $\Phi$ -OTDR system can be improved to 9.41 dB, 9.02 dB, 7.60 dB, and 3.50 dB, under the fault positions of 2.3, 5.0, 10.8, and 16.0 km, respectively, along the cable link. The SNR of the  $\Phi$ -OTDR system under the fault position of 2.3 km is further improved when  $N=8$  and the peak value of the frequency band RSMD highlighted the weak fault position, which is a little different from the actual situation. Combining both algorithms can reduce the signal processing time and the weak fault location accuracy along the optical-fiber link to  $\pm 2$  m. Additionally, the proposed algorithm improves the SNR of the  $\Phi$ -OTDR optical cable link fault detection signal in the UHV DC control and protection engineering system, which identifies weak faults along the optical cable link and realizes the accurate positioning of weak fault events.

**Key words** fiber optics; ultra-high voltage (UHV); DC control and protection; phase-sensitive optical time domain reflectometer ( $\Phi$ -OTDR); signal-to-noise ratio (SNR)